



PI-Fuzzy Control Applied to the Hybrid PV / Wind Pumping System with Energy Storage

Ahmed Medjber¹, Abdelhafidh Moualdia^{2*} and Abdelkader Morsli²

¹ *LSEA, Research Laboratory of University of Medea, Algeria.*

² *Laboratory of Electrical Engineering and Automatics (LREA), University of Medea, Algeria.*

Received: September 8, 2021; Revised: June 15, 2022

Abstract: The aim of this paper is to develop an autonomous hybrid energy management algorithm method with storage (lead-acid type battery bank), applied to the hybrid pumping system capable of ensuring the level regulation of water in the tank. The designed system is composed of a photovoltaic generator, connected to a booster chopper, a DC bus and a wind power system driving a permanent magnet synchronous generator. Two control strategies were implemented. The first, based on P and O, ensures the operation of the GPV with its maximum power via the control of a booster chopper. The second was applied to the turbine to extract the maximum power from the wind (MPPT). Two PI and fuzzy controllers to drive the operation of the asynchronous motor driving the centrifugal pump controlled the mechanical speed and the magnetic flux. In addition, we have established an explicit relation making it possible to adopt the set point rotation speed of the asynchronous machine and consequently, the pump output according to various climatic conditions. The results obtained show the validity, efficiency and robustness of the various techniques developed.

Keywords: *centrifugal pump; hybrid energy; fuzzy logic control; PMSG.*

Mathematics Subject Classification (2010): 03B52, 93C42, 94D05.

* Corresponding author: <mailto:amoualdia@gmail.com>

1 Introduction

The most common renewable energy sources for agricultural applications are solar energy and wind energy; photovoltaic pumping usually consists of solar panels, a control unit and a pump set. Depending on the sizing of the system, it is sometimes necessary to use storage batteries and a charge regulator (due to the intermittent nature of solar radiation). This makes it possible to avoid problems of adaptation between the photovoltaic generator and the pump set. However, it is better to store water in a tank rather than storing energy in batteries. The use of wind turbines to pump water is not new. Wind power is one of the most promising sources for water pumping applications. Recent and relevant research on wind pumping applications shows that:

- Wind power based water pumping systems are best suited for irrigation applications [1];
- It is an economically viable alternative technology for irrigation systems [2];
- The wind power system can be used successfully for groundwater pumping in remote areas, where wind resources are available [3].

Moreover, a comparative study between photovoltaic and wind power systems for water pumping systems in the Sahara regions was carried out in Algeria [4]. It emerges from this study that the cost per cubic meter of water produced by the wind pumping system is less expensive than that produced by the photovoltaic system. Over the past decade, very few studies have been done on hybrid renewable energy systems for pumping water, unlike systems on their own [4]. Hybrid systems designed to work in agricultural applications are more flexible and reliable, it is also concluded that hybrid pumping systems are suitable for small water pumping systems and are of considerable interest for their flexibility . The work presented consists of the modeling, the regulation using PI and fuzzy regulators and the optimization of a hybrid wind-photovoltaic energy system not connected to the electricity grid. The work aims mainly to bring to the energy management of hybrid autonomous systems with renewable energies with storage for agricultural applications in tropical environments, then we will present the results obtained comparatively by the fuzzy regulator and PI.

2 Modeling of the Hybrid Pumping System

Figure 1 shows the complete diagram of hybrid power generation. The system consists of a wind power system assisted by PMSG, a PV system assisted by MPPT technique, a water pump assisted by ASM and an energy management system.

2.1 Wind turbine model

The power of the wind is defined by [5]

$$P = 0.5 \rho A V^3, \quad (1)$$

where ρ is the density of the area, A is the circular area (m^2), V is the wind speed in (m/s). The aerodynamic power produced by the turbine can be expressed by

$$P_m = 0.5 C_p(\lambda, \beta) \rho A V^3, \quad (2)$$

$$\lambda = \frac{R \cdot \Omega_{tur}}{V},$$

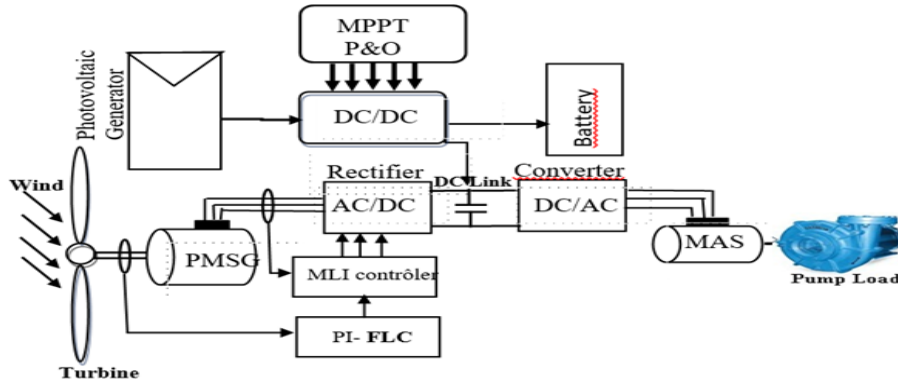


Figure 1: The block diagram of the hybrid water pumping system.

where C_p is the power coefficient, λ is the speed ratio, β is the blade pitch angle, Ω_{tur} is the turbine rotation speed (rd/s). The power coefficient can be expressed by

$$C_p(\lambda, \beta) = 0.5176 \left(\frac{116}{\lambda_i} - 0.4\beta - 5 \right) e^{\frac{1}{\lambda_i}} + 0.0068 \lambda, \quad (3)$$

$$\frac{1}{\lambda_i} = \frac{1}{\lambda + 0.08\beta} - \frac{0.035}{\beta^3 + 1}.$$

The aerodynamic torque is defined by

$$T_{aero} = \frac{P_{aero}}{\Omega_{tur}} = \frac{0.5 C_p(\lambda, \beta) \rho A V^3}{\Omega_{tur}}. \quad (4)$$

The fundamental dynamic equation of the tree is described by the following equation:

$$J \frac{d\Omega}{dt} = T_{aero} - T_{em} - f\Omega, \quad (5)$$

$$J = \frac{J_{tur}}{G^2} + J_g,$$

where T_{em} is the electromagnetic torque produced by the generator, T_{aero} is the turbine torque, f is the friction of the turbine rotor. J is the total inertia.

2.2 Model of the permanent magnet synchronous machine PMSG

The stator voltage equations dq of this generator are given by the following expressions [6]:

$$L_d \frac{di_d}{dt} = V_d - R_s i_d + L_q \omega i_q,$$

$$L_q \frac{di_q}{dt} = V_q - R_s i_q - L_d \omega i_d + \varphi_f, \quad (6)$$

$$\varphi_d = L_d i_d + \varphi_f \quad \varphi_q = L_q i_q.$$

The electromagnetic torque is represented by [7, 8]

$$T_{em} = \frac{3}{2} p [(L_d - L_q) i_d i_q + i_q \varphi_f], \quad (7)$$

where p is the number of pole pairs. The PMSG is assumed to be a wound rotor, and the expression of the electromagnetic torque in the rotor can be described as follows:

$$T_{em} = \frac{3}{2} p \varphi_f. \quad (8)$$

2.3 Asynchronous machine model

The ASM modeling is represented by the following equations [9, 10]:

$$\begin{aligned} V_{ds} &= R_s i_{ds} + L_s \frac{di_{ds}}{dt} + M \frac{di_{dr}}{dt} - L_s \omega_s i_{qs} - M \omega_s i_{qr}, \\ V_{qs} &= R_s i_{qs} + L_s \frac{di_{qs}}{dt} + M \frac{di_{qr}}{dt} - L_s \omega_s i_{ds} - M \omega_s i_{dr}, \\ V_{dr} &= 0 = R_r i_{dr} + L_r \frac{di_{dr}}{dt} + M \frac{di_{ds}}{dt} - L_r \omega_r i_{qr} - M \omega_r i_{qs}, \\ V_{qr} &= 0 = R_r i_{qr} + L_r \frac{di_{qr}}{dt} + M \frac{di_{qs}}{dt} - L_r \omega_r i_{ds} - M \omega_r i_{dr}. \end{aligned} \quad (9)$$

Using the orientation of the rotor flux towards the d-axis equation 6 and substituting for the magnetic flux equations and the equations from 9, the differential equations of ASM can be obtained as follows:

$$\varphi_{dr} = \varphi_r, \quad \varphi_{qr} = 0, \quad \sigma = 1 - \left(\frac{M^2}{L_s L_r} \right) \quad T_r = \frac{L_r}{R_r}, \quad (10)$$

$$V_{ds} = (R_s + L_s P) i_{ds} - \left(\omega_s L_s \sigma i_{qs} - \frac{M}{L_r} \frac{d\varphi_r}{dt} \right) = V_d^* - e_q, \quad (11)$$

$$V_{qs} = (R_s + L_s P) i_{qs} + \left(\omega_s L_s \sigma i_{ds} + \frac{M \omega_s}{L_r} \varphi_r \right) = V_q^* + e_d, \quad (12)$$

$$i_{ds}^* = (1 + T_r P) \frac{1}{M} (\varphi_{dr} - \varphi_{dr}^*), \quad i_{qs}^* = \frac{L_r C_{em}^*}{p M \varphi_{dr}^*}. \quad (13)$$

The resistant torque is defined as follows:

$$C_r = k \cdot \Omega. \quad (14)$$

2.4 Current model

The output of the speed regulator makes it possible to generate the reference current which is compared to the value of the current from the measurement of the real currents in Figure 2 and their error applied to the input of the current regulator. In parallel with this loop, there is a current regulation loop i_d , which is kept constant corresponding to the output of the flow regulator [12]. The outputs of the current regulators are applied to a decoupling block which generates reference voltages, and by the inverse Park transformation, we obtain the voltages which are the voltages of the inverter control with PWM control, i_{ds} , i_{qs} , V_{ds} and V_{qs} .

2.5 Photovoltaic generator model

To size the capacity of the system and predict the power of the PV generator, there are several energy models that take into consideration E_t (W/m^2), the solar radiation and

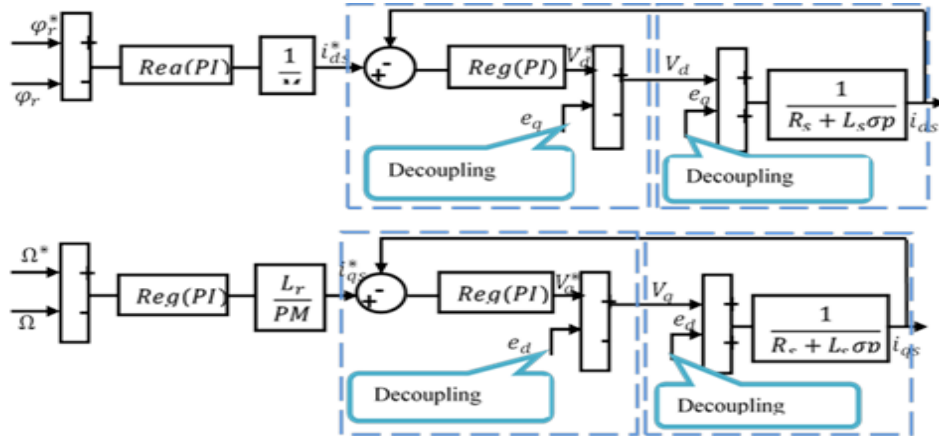


Figure 2: Block diagram of the currents including the MAS compensation terms.

the $A(m^2)$ surface of the panel which is given as follows [13]:

$$P_{PV} = N_{PV} \cdot A \cdot E_t, \tag{15}$$

$$N_{PV} = N_r \cdot N_{PC} + [1 - \beta (T_C - T_{C-ref})], \tag{16}$$

$$T_C = T_a \left[\frac{NOCT - 40}{1000} \right] \cdot E_t. \tag{17}$$

N_{PV} represents the efficiency of the PV generator, N_r is the efficiency of the reference module, NOCT is the nominal operating temperature of the cell, N_{PC} is the efficiency of the power conditioning, T_{C-ref} is the reference cell temperature ($degC$) and T_C is the cell temperature that can be calculated as in [14].

To achieve the desired pump power, the PV system is made up of $N_s = 12$ panels in series and $N_p = 2$ panels in parallel.

2.6 Centrifugal pump model

The sizing of a pumping system is according to field conditions, but the choice of the pump (centrifugal pump) is according to the real characteristics of the installation in which it is to be installed [15]. The following data will be required to size the pump: the water flow $Q(m^3/h)$ and the total anemometry head HMT. HMT is given as follows:

$$HTM = H_g + \Delta H = (H_{ga} + H_{gr}) (1 + PC), \tag{18}$$

where ΔH are the head losses in the installation, H_{ga}, H_{gr} are the height of respiration and discharge, PC is the pipe loss = 10% for $H_{ga} = H_{gr} = 7m$, then $HMT = 15.4m$. For 3 hectares of agricultural land and 56 people, the water needs of the installation considered are estimated at $200m^3/day$, The pump operates 3 hours/day, we will have $Q = 0.185m^3/s$. The hydraulic power is defined by

$$P_H = \rho g H Q = 2.8 kW. \tag{19}$$

The efficiency of the pump type *NM4125/250 CALPEDA* is 78%, the number of revolutions $n = 1450tr/min$.

$$\eta = \frac{P_H}{P_{mec}} \implies P_{mec} = \frac{P_H}{\eta} = 3.6 kW. \quad (20)$$

The performances (flow Q , height H and power P) are given by

$$\frac{Q}{Q_{ref}} = \frac{\Omega}{\Omega_{ref}}, \quad (21)$$

$$\frac{H}{H_{ref}} = \left(\frac{\Omega}{\Omega_{ref}} \right)^2, \quad (22)$$

$$\frac{P}{P_{ref}} = \left(\frac{\Omega}{\Omega_{ref}} \right)^3. \quad (23)$$

3 Hybrid Pumping System Control

The purpose of using an MPPT controller in such a system is to maximize the water flow. The water flow is related to the speed of the asynchronous motor by equation (20) so that maximizing the rotational speed of the motor pump, the group will maximize the water flow, it is doubled by maximizing the power absorbed by the motor which drives the centrifugal pump. The fuzzy logic controller (FLC) is another method used to extract

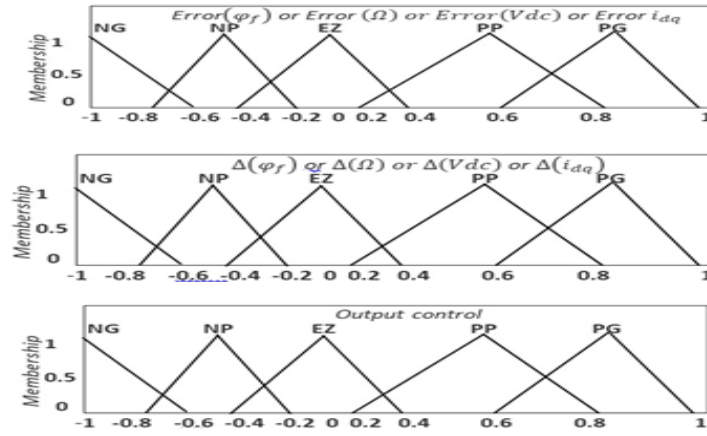


Figure 3: Membership functions for FLC input and output variables.

the maximum power point for either photovoltaic or wind power conversion systems [16, 17]. The FLC has many advantages such as the simplicity of designing it without any knowledge of the characteristics of the system, its high performance with lower oscillation around the point of maximum power, which means increasing the stability of the system, and also having a quick response. The FLC controller applied to the system under study consists of two input variables [18]: the first input variable is the mechanical speed error of MAS or the magnetic flux error as shown in the figure, the second is the variation of the error, the inputs of the FLC can be calculated as follows:

$$E_{\Omega} = \Omega_{ref} - \Omega, \quad E_{\varphi} = \varphi_{f-ref} - \varphi_f, \quad E_{V_{dc}} = V_{dc-ref} - V_{dc}, \quad \Delta E = \frac{dE}{dt}. \quad (24)$$

Table 1: Inference matrix.

Error for $\varphi_f, V_{dc}, \Omega$ and i_{dq}	output control				
	NG	NP	EZ	PP	PG
NG	PG	PG	NG	NP	NG
NP	PG	PP	NP	NP	NG
EZ	NP	NP	EZ	PP	PP
PP	NG	NP	EZ	PP	PG
PG	NG	NG	NP	PG	PG

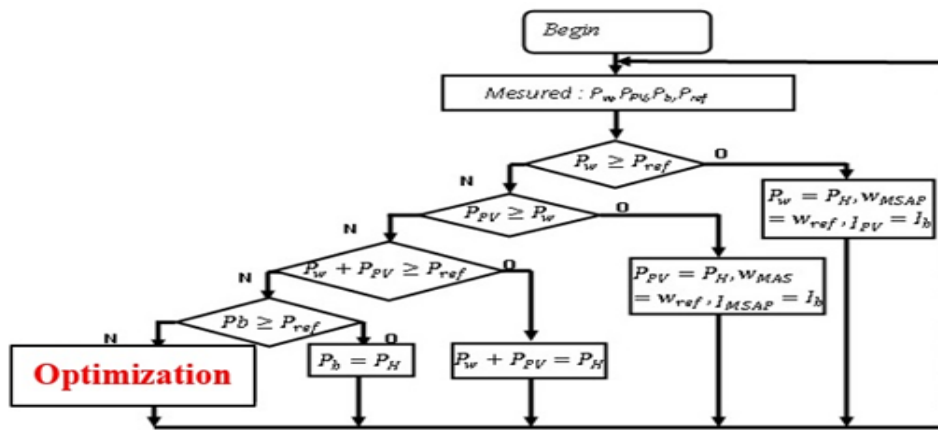


Figure 4: Hybrid management organization chart.

4 Simulation Results and Discussion

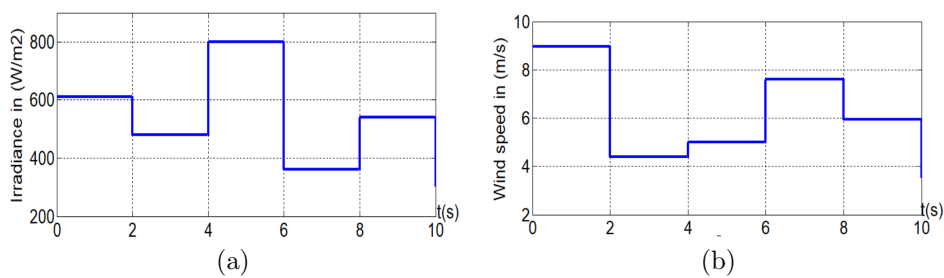


Figure 5: (a): Solar radiance, (b): Wind profile.

The evolution of the weather conditions influences the characteristic of the asynchronous machine and, consequently, the performance of the pump, the results obtained show the performance of the PI-Flow controllers and of the vector control applied to the

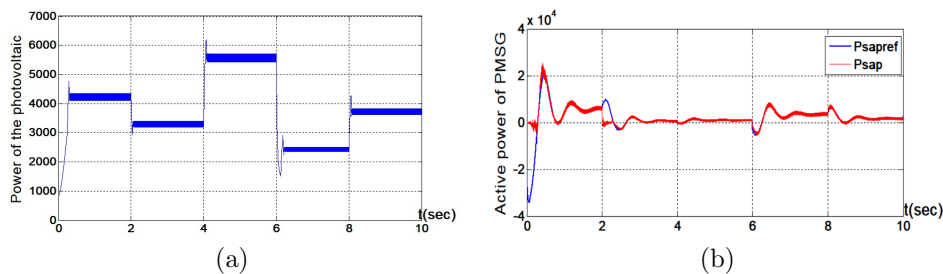


Figure 6: (a): Power of the photovoltaic panel, (b): Active power of the PMSG.

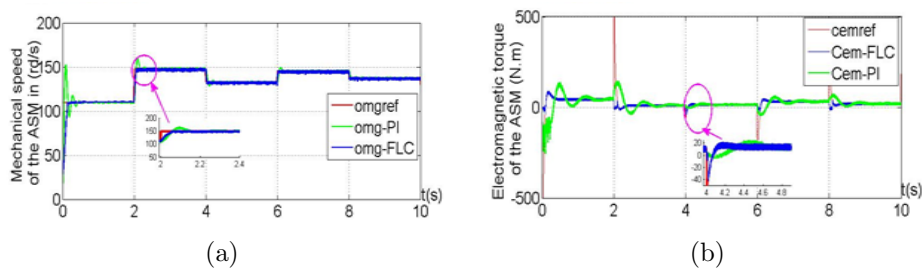


Figure 7: (a): Mechanical speed of the ASM, (b): Electromagnetic torque of the ASM.

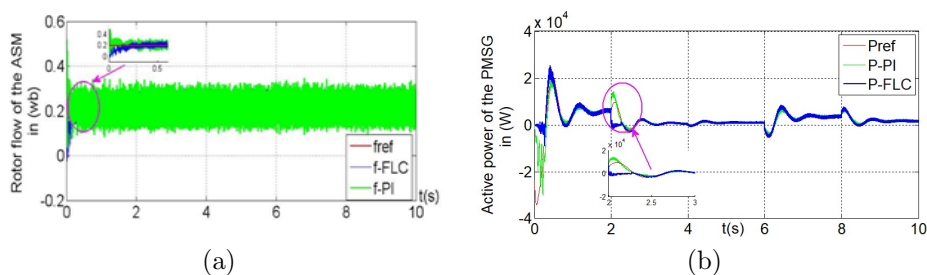


Figure 8: (a): Rotor flow of the ASM, (b): Active power of the PMSG.

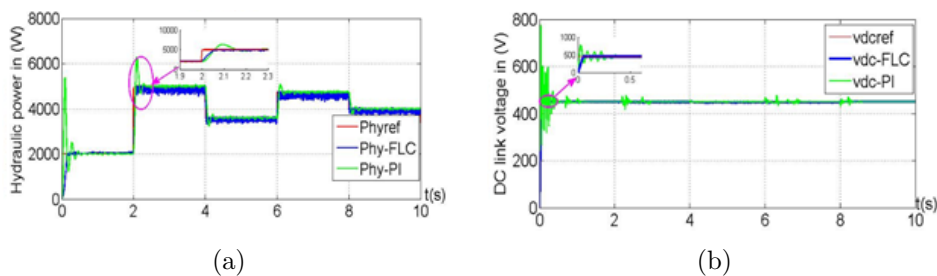


Figure 9: (a): The Hydraulic power of the pump, (b): DC link voltage.

ASM, we consider, in this simulation, the evolution of the hydraulic power requested, see Figure 9(a), according to the above results, we notice that at an instant less than 2s, the wind speed is important, while the solar irradiation is low as shown in Figures 5(a) and

5(b), then the power is generated by the wind generator, see Figure 6(b), depending on the speed of the wind, the management system makes the power system to operate the pump as shown in Figure 11(b), and takes advantage of the energy supplied by the PV generator to recharge the battery, see Figure 11(a). The increase in the state of charge of the battery, see Figure 12, and at the instant between 2s and 4s, the available power (PV and wind turbine) is insufficient to satisfy the need for water, and at this moment, the pump operates from the battery, see Figure 11(b), this results in the reduction of the state of charge of the battery, see Figure 12, for the moment between 4s and 6s, at the strong solar irradiation but the weak wind, in this case, the energy of the PV generator is injected into the motor pump, see Figure 11(b), and exploiting the current produced by the wind turbine to recharge the battery as shown in Figure 11(a), subsequently, the PV and wind power is less than the hydraulic power, but the sum is greater.

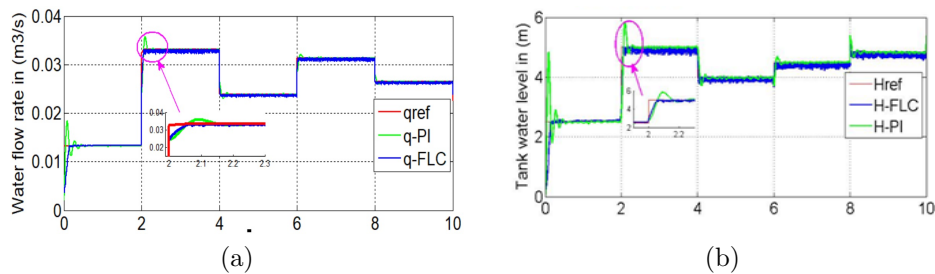


Figure 10: (a): Water flow rate, (b): Tank water level.

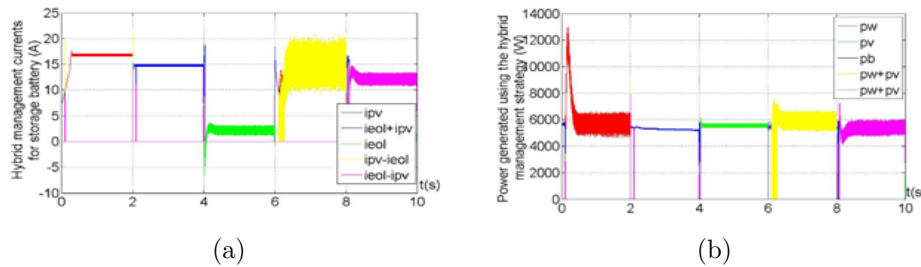


Figure 11: (a): Hybrid management currents for charging and discharging the storage battery, (b): Power generated using the hybrid management strategy.

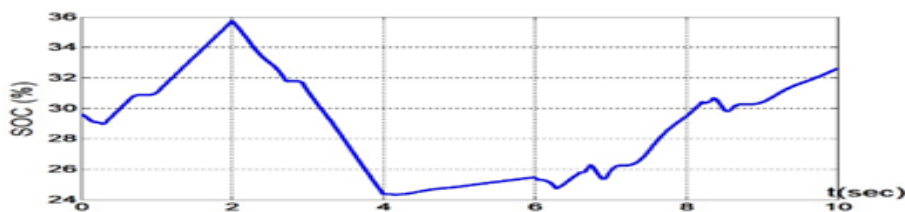


Figure 12: The state of charge and discharge of the battery.

In this case, the photovoltaic energy, as well as that produced by the wind turbine, is used to drive the motor pump, and the excess energy is sent to the battery, which leads to an increase in the state of charge of the battery, see Figure 11(b) and Figure 12, therefore, the electrical and mechanical reference quantities have been well followed by the pump set, clearly showing the fuzzy regulator performance, PI and vector control by the orientation of the rotor flux applied to the machine, thus the efficiency of the MPPT adapter. The response time obtained by the FLC controller is considerably reduced, the peak overrun values are limited as compared to the PI controller, the tank water level, see Figure 10(b), the water flow, see Figure 10(a) as well as the pump power, see Figure 9(a) follow their reference values successfully thanks to the hybridization of photovoltaic-wind energy, hence the satisfaction of daily water needs.

5 Conclusion

The main objective of this paper was to develop a complete model of the photovoltaic-wind hybrid system with storage applied to the pumping system, from this model; an energy management strategy was developed and analyzed. We then chose the strategy that allows maintaining both the state of charge of the batteries and the water level of the tank. To achieve our objective, we presented the modeling of the various components of the system, a good dimensioning of the storage allowed us to ensure the energy needs requested by the pump. Subsequently, we were able to optimize the system under study to guarantee the daily water requirements requested. In order to exploit the photovoltaic generators and the wind power to the maximum, the simulation results show the performance of fuzzy regulator and the vector control applied to the asynchronous machine having for principle, the decoupling between the torque and the flux. These tests in weather conditions show the efficiency of hybridization in a hybrid photovoltaic-wind pumping system to meet daily water needs.

Acknowledgment

The research is part of a project PRFU'2020, realized, respectively, in the LSEA, Research Laboratory and Laboratory of Electrical Engineering and Automatic LREA Research, University of Medea, Algeria.

References

- [1] A. Adallah and Z. Abdulqader. Performance analysis of a hybrid wind/photovoltaic power generation system for water pumping. *Springer, International Journal of Environmental Science and Technology* **16** (2019) 5295–5304.
- [2] G. Misrak, M. Marta and A. Abebayehu. Feasibility study of a wind powered water pumping system for rural Ethiopia. *AIMS Energy* **3** (4) (2015) 851–868.
- [3] Y. Chedni, Dj. Boudana, A. Moualdia, L. Nezli and P. Wira. Sensorless Two Series Connected Quasi Six-Phase IM Based Direct Torque Control for Torque Ripples Minimization. *Nonlinear Dynamics and Systems Theory* **20** (2) (2020) 153–167.
- [4] A. Moualdia, M. O. Mahmoudi and L. Nezli. Direct Torque Control of the DFIG and Direct Power Control for Grid Side Converter in wind power generation system. *The Mediterranean Journal of Measurement and Control, MEDJMC* **9** (3) (2013) 101–108.

- [5] S. Boulkhrachef, A. Moualdia, Dj. Boudana and P. Wira. Higher-order sliding mode control of a wind energy conversion system. *Nonlinear Dynamics and Systems Theory* **19** (4) (2019) 486–496.
- [6] A. G. Mazko. Robust output feedback stabilization and optimization of discrete-time control systems. *Nonlinear Dynamics and Systems Theory* **18** (1) (2018) 92–106.
- [7] T. Djellouli, S. Moulahoum, A. Moualdia, M. S. Bouchrit and P. Wira. Speed Sensorless Direct Torque Control Strategy of a Doubly Fed Induction Motor Using an ANN and an EKF. *Nonlinear Dynamics and Systems Theory* **20** (4) (2020) 374–387.
- [8] A. Ansari and D. M. Deshpande. Mathematical Model of Asynchronous Machine in MATLAB Simulink. *International Journal of Engineering Science and Technology* **2** (5) (2010) 1260–1267.
- [9] E. Benyoussef, A. Meroufel and S. Barkat. Neural network and fuzzy logic direct torque control of sensorless double star synchronous machine. *Rev. Roum. Sci. Techn. Electrotechn. and Nerg.* **61** (3) (2016) 239–243.
- [10] S. Bentouati, A. Tlemcani, N. Henini and H. Nouri. Adaptive Sliding Mode Control Based on Fuzzy Systems Applied to the Permanent Magnet Synchronous Machine. *Nonlinear Dynamics and Systems Theory* **21** (5) (2021) 457–470.
- [11] A. Chalanga, S. Kamal and B. Moreno. Implementation of super-twisting control: super-twisting and higher order sliding-mode observer-based approaches. *IEEE Trans. on Industrial Electronics* **63** (6) (2016) 3677–3685 .
- [12] A. E. Leon and J. A. Solsona. Sub-Synchronous Interaction Damping Control for DFIG Wind Turbines. *IEEE Transactions on Power Systems* **30** (1) (2015) 419–428.
- [13] L. Wang, M. Zhao, X. Wu, X. Gong and L. Yang. Fully integrated high-efficiency high step-down ratio DC/DC buck converter with predictive over-current protection scheme. *IET Power Electronics* **10** (14) (2017) 1959–1965.
- [14] A. Ajami, H. Ardi and A. Farakhor. Design, analysis and Implementation of a Buck-Boost DC/DC Converter. *IET Power Electronics* **7** (12) (2014) 2902–2913.
- [15] T. Ramji and N. Ramesh Babu. Fuzzy logic based MPPT for permanent magnet synchronous generator in wind energy conversion system. *IFAC-Papers* **49** (1) (2016) 462–467.
- [16] N. Khattab, M. Badr, E. El Shenawy, H. Sharawy and M. Shalaby. Feasibility of Hybrid Renewable Energy Water Pumping System for a Small Farm in Egypt. *International Journal of Applied Engineering Research* **11** (11) (2016) 7406–7414.
- [17] A. Gholamshahi and R. Fadaeinedjad. A New Control Strategy for Hybrid Water Pumping Systems Used by Utilities in Developing Countries *IEEE* (2019) 2406–2413.
- [18] A. Nekkache, B. Bouzidi and S. Ait-Cheikh. Optimal Sizing of Hybrid PV/Wind Based Water Pumping System Considering Reliability and Economic Aspects. In: *International Conference on Wind Energy and Applications in Algeria (ICWEAA)*, 2018.
- [19] L. Stoyanov, I. Bachev and Z. Zarkov. Multivariate Analysis of a Wind/PV-Based Water Pumping Hybrid System for Irrigation Purposes *Energie* **14** (2021) 3231–3246.
- [20] J. C. Rosa, S. Uranio and N. Diana. Design and Performance of Photovoltaic Water Pumping Systems: Comprehensive Review towards a Renewable Strategy for Mozambique. *Journal of Power and Energy Engineering* **6** (2018) 32–63.
- [21] T. Aized, M. Syed and K. Sajid. Design and analysis of wind pump for wind conditions in Pakistan. *Advances in Mechanical Engineering* **9** (11) (2019) 1–18.